Effect of discontinuity dip direction on hard rock pillar strength

K.V. Jessu
WA School of Mines, Curtin University, Australia

T.R. Kostecki
Southern Illinois University, Carbondale, IL, USA

A.J.S. Spearing
WA School of Mines, Curtin University, Australia

G.S. Esterhuizen
National Institute for Occupational Safety and Health, Pittsburgh, PA, USA

Abstract

Discontinuities are geologic occurrences in rock and when present within a pillar, reduce the strength of the pillar. Empirical formulas that are commonly used to determine pillar strength do not explicitly take into account the presence of discontinuities and thus can overestimate the pillar strength. The effect of discontinuities on the strength of pillars has been investigated using numerical models, but in these models, the discontinuity strike was parallel with the pillar faces. In this study, fully three-dimensional hard rock pillars were simulated using numerical modeling to understand the effect of the discontinuity dip direction on square and rectangular hard rock pillars. Based on the results, recommendations to assess a pillar's strength in the presence of a discontinuity are discussed.

Key words: Hard rock pillar, Discontinuity, Rectangular pillars

2018 *Transactions of the Society for Mining, Metallurgy & Exploration,* Vol. 344, pp. 25-30.
https://doi.org/10.19150/trans.8745

Introduction

Discontinuities are an integral part of rock strata and create potential support and stability problems both during and after mine development. These discontinuities exist as discrete planes in a rock-mass where sliding movement may or may not occur. The strength of a rock sample with the presence of a discontinuity is significantly less than the strength of the intact rock sample, depending on its orientation relative to the stress direction (Jaeger and Cook, 1979). Pillars have been shown to behave similarly to a rock sample, suggesting that the strength of the pillar also depends on the discontinuity present in the pillar (Esterhuizen, 2006). To illustrate this concept of pillars with discontinuities, an example of a limestone pillar intersected by a major structural feature is shown in Fig. 1.

Empirical equations for designing pillars are all based on examining stable, unstable and failed pillars without giving much emphasis to the mode of failure. Therefore, in the presence of a major discontinuity, if the pillar is designed using empirical approaches such as Lunder and Pakalnis (1997), the pillar strength can be overestimated. Abrupt pillar failure due to the presence of a discontinuity will increase the amount of load on the adjacent pillars and can lead to chain pillar failures, especially if the system has a low factor of safety.

Early studies, mainly by Madden et al. (1995) in the South African Coal Fields, showed that discontinuities had a significant effect on the strength of the pillars. As a result, a pillar condition rating system was introduced to better estimate the pillar strength. This system cannot be adopted as a "universal" design since the rating system is based mainly on visual inspection of fracturing, scaling of the pillars and other visual tell-tales of the pillar condition, and because its empirical database is limited to coal pillars observed in South Africa.

Later studies by Iannacchione (1999) of limestone pillars showed a relationship between the dip angles of discontinuities relative to the pillar strength, and concluded that pillar strength is most significantly affected by discontinuity dip

Paper number TP-17-015. Original manuscript submitted April 2017. Revised manuscript accepted for publication February 2018. Discussion of this peer-reviewed and approved paper is invited and must be submitted to SME Publications Dept. prior to Sept. 30, 2019.

angle at 60°. Two studies incorporating numerical modelling to study pillars intersected by discontinuities were undertaken by Esterhuizen (1998, 2006). One such study focused on the relationship between pillar strength relative to changes in the dip angle of a discontinuity and varying pillar width-to-height ratios in the limestone mines. The other study focused on slender and squat coal pillars in the presence of a discontinuity.

This paper will present the numerical analysis of a discontinuity oriented at 45° to the pillar face at different dip angles and varying pillar width-to-height ratios. The orientation of the discontinuity to that of the rectangular pillars is also investigated.

Dip direction/strike. In previous studies, the numerical models using FLAC^{3D} and UDEC were evaluated with the dip directions (strike) parallel to that of the face of the pillar, as shown in Fig. 2a. Esterhuizen, Dolinar and Ellenberger (2008) accounted for the effect of discontinuities on pillar strength in limestone mines as follows:

$$S = 0.65 * UCS * LDF * \frac{w^{0.30}}{h^{0.59}} \quad (1)$$

where *UCS* is the uniaxial compressive strength of the intact rock, 0.65 represents the reduction of limestone *UCS* strength, *w* and *h* are the width and height of the pillars, and *LDF* is the large discontinuity factor. The large discontinuity factor is derived from the numerical models and given as:

$$LDF = 1 - DDF * FF \quad (2)$$

where *DDF* is the discontinuity dip factor and depends on both the discontinuity dip and the pillar width-to-height ratio, and *FF* is the frequency factor — that is, the number of large discontinuities per pillar. The *DDF* was developed with the numerical models only based on the discontinuity dip direction of 0° as shown in Fig. 2a.

Obviously, different discontinuity dip directions (strike) can be encountered in the mine to that of the pillar face. A limited study conducted by Esterhuizen (1998) with multiple discontinuities having a dip of 60° and dip direction of 45° to that of the pillar face concluded that the strength obtained was 10 percent less than that to the multiple discontinuities parallel — that is, dip direction = 0° — to the pillar face. This approach can be used with a single discontinuity to understand the strength of the pillars at different dip directions and different dip angles, as shown in Fig. 2.

Figure 1 — Example of pillar with major structural feature (Esterhuizen, 2006).

Rectangular pillars. Rectangular pillars can be effective in increasing pillar strength and have been suggested by several researchers (Wagner, 1992; Mark and Chase, 1997; Galvin, Hebblewhite and Salamon, 1999; Dolinar and Esterhuizen, 2007). An equivalent width method was introduced by Wagner (1992) and further modified by Esterhuizen, Dolinar and Ellenberger (2008), taking into consideration the confinement effect, and is given as:

$$w_e = w + \left(\frac{4A}{C} - w\right) * LBR \quad (3)$$

where *w* is the width of the pillar, *A* is the area of the pillar, *C* is the circumference of the pillar, and *LBR* is the length benefit ratio, which increases from 0 to 1 with increasing width-to-height ratios. However, this equation does not take into account the structural features and direction of pillar length relative to discontinuity such that the pillar strength increases.

Model configuration for this study

FLAC^{3D} (Itasca Consulting Group, 2016), a finite difference geotechnical software, was used to investigate the strength of the pillars in the presence of the discontinuity, as it has a capability to model the realistic failure process of

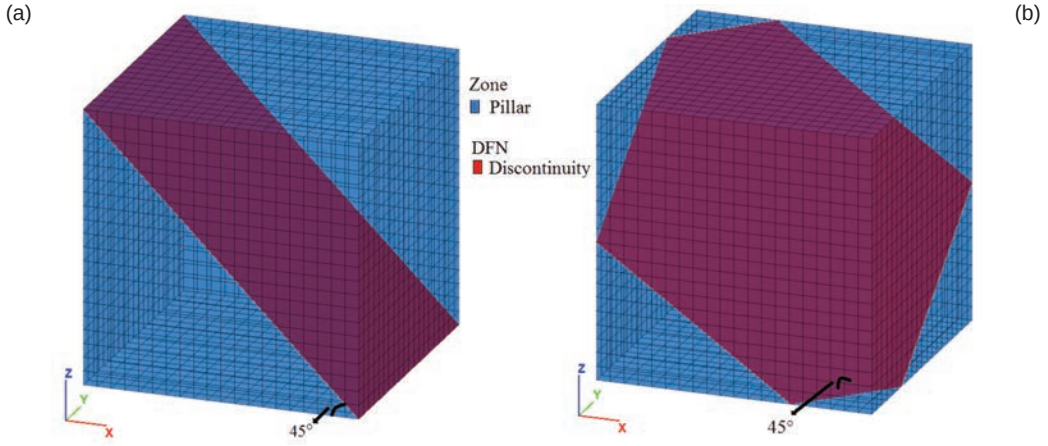

Figure 2 — Discontinuity with 45° dip with dip direction of (a) 0° and (b) 45°.

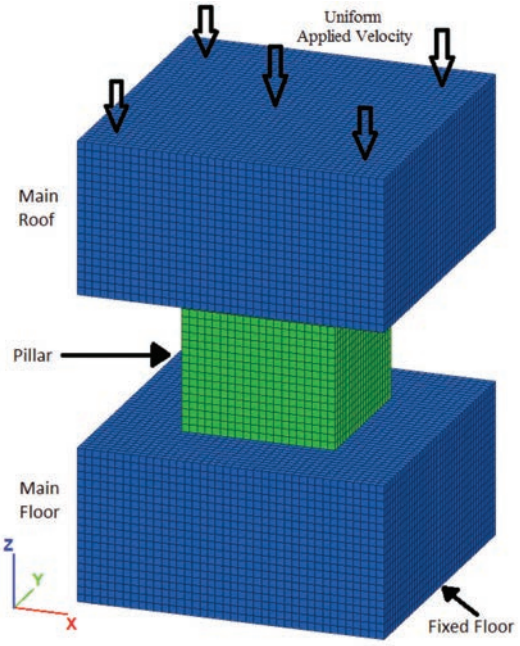

Figure 3 — FLAC^{3D} pillar model.

Table 1 — Model properties (Dolinar and Esterhuizen, 2007).

Rock mass properties	Numerical value
Bulk modulus	40,000 MPa
Shear modulus	24,000 MPa
Intact rock strength (UCS)	150 MPa
Cohesion (brittle)	25 MPa
Friction (brittle)	0°
Cohesion (Mohr-Coulomb)	8.1 MPa
Friction (Mohr-Coulomb)	47.6°
Tension	2.7 MPa
Dilation	30°

Table 2 — Joint properties (Dolinar and Esterhuizen, 2007).

Joint properties	Numerical value
Joint cohesion	1 MPa
Joint friction	42°
Joint tension	0.4 MPa
Joint dilation	0°

hard rock pillars (Esterhuizen, 2006). The coordinate system in the horizontal plane is represented by *x*- and *y*-directions and in the vertical plane by the *z*-axis, as shown in Fig. 3. The model consists of the main roof, main floor, and pillar with width *W* and height *H*. The height of the pillar and the extraction ratio of 75 percent were kept constant while the pillar and the entry width were varied to simulate different width-to-height ratios.

Boundary and loading conditions. The bottom of the floor was fixed such that the displacements and the velocities are restricted in the normal and parallel directions. The roller boundaries were incorporated in the *x*- and *y*-plane such that the displacements and the velocities are restricted in the normal direction. The simulation of the pillar under compression was carried out by subjecting the top of the main roof to the applied velocity.

The model was subjected to a vertical stress of 2.7 MPa, which simulates a mine of depth 100 m with a vertical to horizontal stress ratio of 1:1 and was run to equilibrium under the elastic conditions. After reaching equilibrium, the pillar material was then transformed from elastic to the sub-ubiquitous (bilinear), and the DFNs were introduced as the single discontinuity in the model. This shows that the rock mass behaves as elastic before excavation, and after excavation the rock mass obtains the properties of brittle and plastic deformation. The model was then subjected to increasing vertical load until the pillar had completely failed and reached the residual strength of about half the peak strength (Esterhuizen, 2006). A FISH function was generated to observe the stress-strain curve from which the average stress at failure could be observed. FISH is a language used within FLAC^{3D} mainly to implement user-defined functions and variables beyond the traditional code in FLAC^{3D}.

Model properties. Brittle rock failure has evolved into an important and better-understood phenomena in rock mechanics. As the stress state in the pillar reaches about 0.3 to 0.5 times the uniaxial compressive strength, brittle cracks develop parallel to the major principal stress. It was necessary to simulate this phenomenon before the shear failure of the rocks. Therefore, the bilinear strength envelope was used in which the strength is independent of friction and is equal to 0.3 to 0.5 times the uniaxial compressive strength at low confinement, then followed by friction hardening at higher confinement (Kaiser et al., 2000).

The sub-ubiquitous model (bilinear strain softening/hardening model), FLAC^{3D} code is capable of simulating the bilinear rock strength based on the Mohr-Coulomb strength criterion and strain softening as a function of the deviatoric plastic strain (Itasca Consulting Group, 2016). The properties for the model with rock mass having a rock mass rating (RMR) of 70 were taken from Dolinar and Esterhuizen (2007) and are shown in Tables 1 and 2 (Esterhuizen, 2006). This model can also incorporate the joints used to evaluate the strength of the pillar in the presence of the discontinuities.

The model element size affects the strain-softening parameters, which should be determined by calibrating the numerical results to that of the theoretical results (Itasca Consulting Group, 2016). All the models were run using identical element sizes. The element size of 0.5 m * 0.5 m * 0.5 m was generated throughout the model and the cohesion softening was carried out to calibrate the results to those of Lunder and Pakalnis (1997).

Model calibration. Intact rock pillar models with width-to-height ratios of 0.5, 0.8, 1.0, 1.2 and 1.5 (the most commonly found W/H ratios in hard rock mines) were generated to validate the numerical models to the theoretical results of Lunder and Pakalnis (1997), as shown in Fig. 4.

The discontinuities dipping at 50°, 60° and 70° with dip direction parallel to the pillar face — that is, strike = 0° — and intersecting the center of the pillar were introduced in

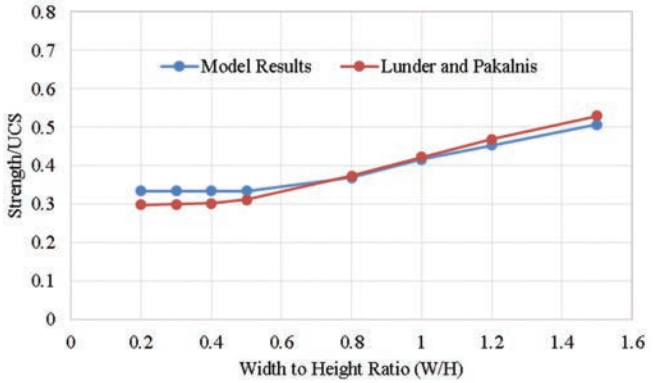

Figure 4 — The numerical models calibrated to the theoretical results of intact rock pillars.

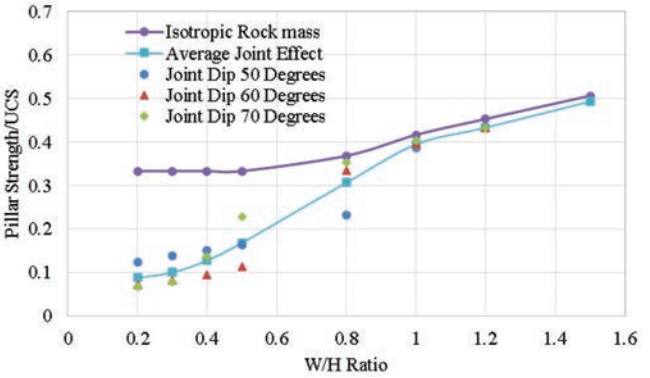

Figure 5 — Results of the numerical models showing the effect of discontinuities dipping at 50, 60 and 70° to the pillar face.

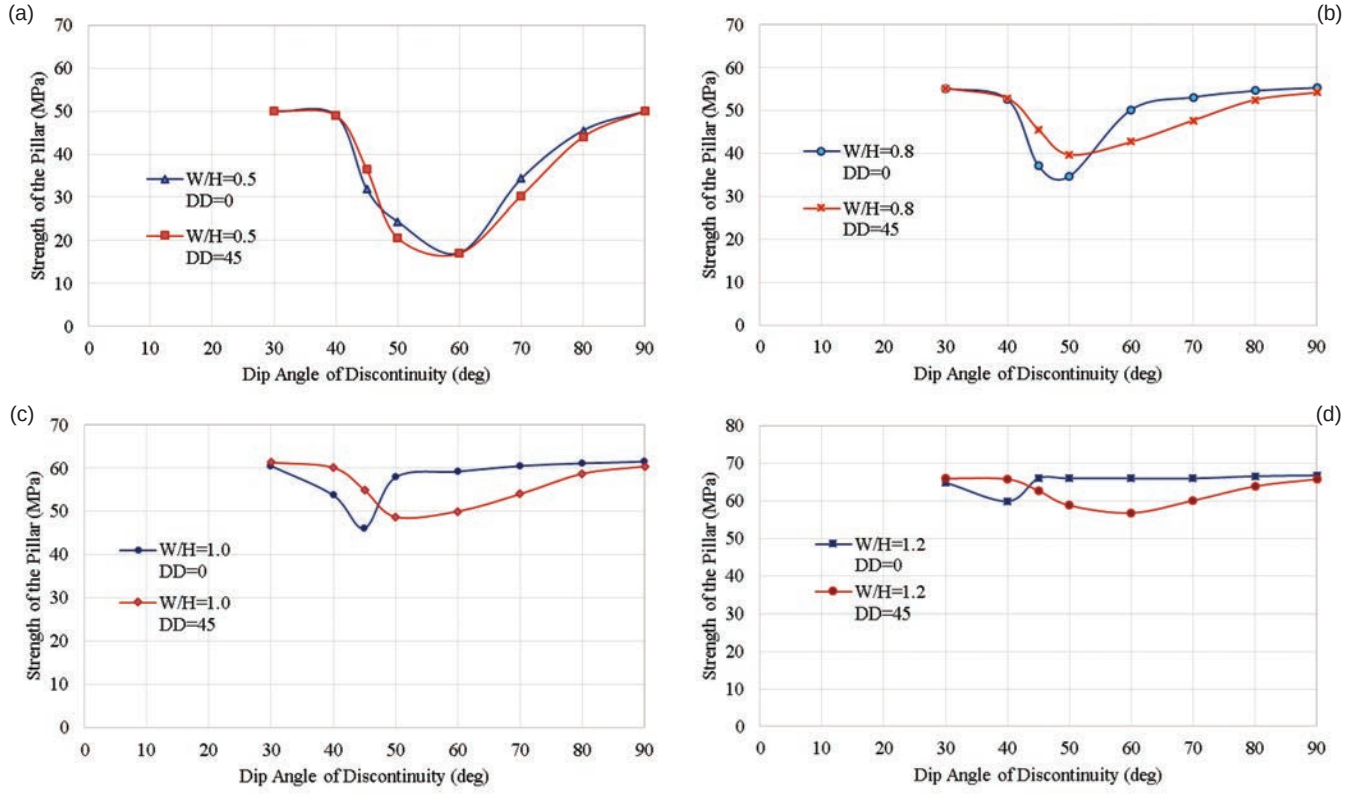

Figure 6 — Effect of the strike of the discontinuity at W/H ratios of (a) 0.5, (b) 0.8, (c) 1.0 and (d) 1.2, where DD = dip direction (strike).

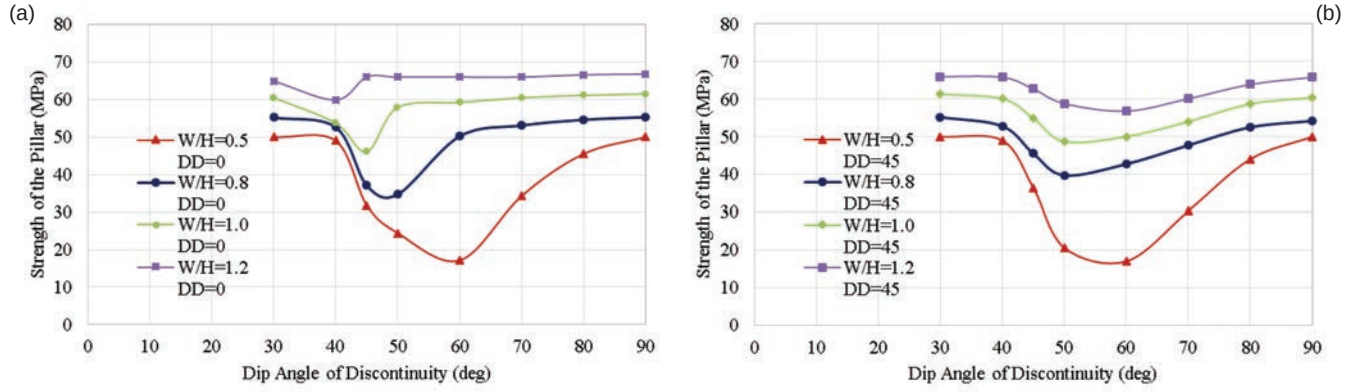

Figure 7 — Effect of discontinuities on pillar strength for strikes of (a) 0° and (b) 45°, where DD = dip direction (strike).

the model and were simulated with varying width-to-height ratios, similar to the results in Esterhuizen (2006), as shown in Fig. 5.

Figure 5 also shows that at higher W/H ratios the discontinuity dip angle has less effect on the strength of the pillars. At a W/H ratio of about 1, the strength of the pillar increases with increasing discontinuity dip angle, such that 70° > 60° > 50°. The strength changes to 70° > 50° > 60° dip angle in the range of a W/H ratio of 0.5 to 0.8, and again changes to 50° > 70° > 60° at a W/H ratio of 0.4. Finally, below a W/H ratio of 0.4, the strength of the pillar decreases with increasing discontinuity dip angle: that is, 50° > 60° > 70°. This shows that the shearing along the discontinuity is the prominent failure to significantly lower the strength of the pillar.

A key parameter is that while simulating continuum models, the pillar strength is not affected by discontinuity dip angle when oriented at angles less than the joint friction angle or at angles nearly perpendicular to the pillar (Jaeger and Cook, 1979). Therefore, the results at the larger angles, larger than 80°, and at very small angles, smaller than 30°, will be near equal to those of the intact pillar strength, which is independent of the discontinuities.

Results and discussion

Evaluating the effect of dip direction/strike. The effect of discontinuity strike non-parallel to the pillar edges was evaluated by simulating two different dip directions, 0° and 45° (Fig. 2), at varying width-to-height ratios and varying dip angles, and the results are shown in Fig. 6. At a W/H ratio of 0.5, the dip direction has little effect on the strength of the pillar. At W/H ratios above 0.5, when the encountered discontinuity dip angles are below 45°, the pillar strength is higher when the discontinuity is oriented at 45° to the pillar face. When the encountered discontinuity dip angles are high, the orientation of the discontinuity parallel to the pillar face leads to higher pillar strength. Therefore, it can be concluded that the dip direction can have a significant effect on the strength of the pillars.

Figure 7 shows the effects of dip angle on the W/H ratio of the pillars with the strike at 0° and 45°. In Fig. 7a, at strike of 0°, the most critical discontinuity dip angle continues to decrease the strength as the W/H ratio increases. In Fig. 7b, at strike of 45°, the most critical discontinuity dip angle falls in the range of 50 to 60° for all W/H ratios considered. It can be thus concluded that when the pillars are designed at the strike angle of 45°, a common strength adjustment factor for all dip angles can be developed to determine the strength of the hard rock pillars.

Rectangular pillars. The rectangular pillars were simulated to investigate the influence of dip direction of the discontinuity. For rectangular pillars, half of the pillar width was added to both sides of the pillar, as shown in Fig. 8, such that the discontinuity passes through the center of the pillar. The pillar length-to-width ratio (L/W) was kept as 2. The lowest strength obtained with the discontinuity dip angle was taken in the rectangular pillars at that W/H ratio — that is, 60° dip angle was used with a W/H ratio of 0.5, 50° dip angle was used with a W/H ratio of 0.8, and 45° dip angle was used with a W/H ratio of 1.0. The dip directions of the discontinuity were varied from 0°, 22.5°, 45°, 67.5° and 90°, as shown in Fig. 9.

Figure 10 shows the effect of dip direction on the rectangular pillars. It can be concluded that the pillar strength is significantly lower when the discontinuity is parallel to the short axis of the pillar. It can be seen that the effect of the discontinuity on pillar strength is limited at dip directions from 0° to 45°. As the discontinuity dip direction is increased above 45°, its effect increases significantly. It can also be seen that the effect of the discontinuity decreases as the W/H ratio increases.

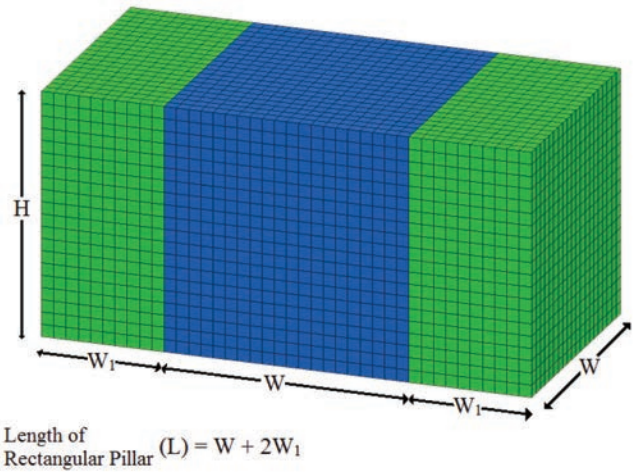

Figure 8 — Formation of the rectangular pillar with L/W ratio of 2.

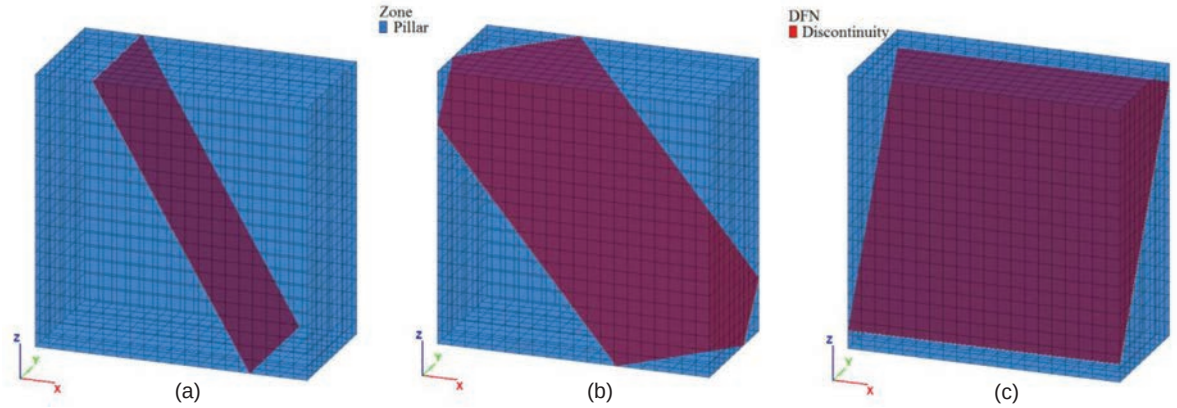

Figure 9 — Rectangular pillar with discontinuity dip angle 60° and dip directions of (a) 0°, (b) 45° and (c) 90°.

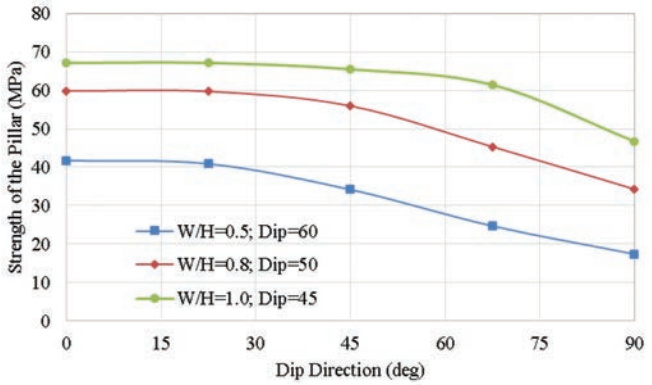

Figure 10 — Effect of dip direction on the rectangular pillars with varying W/H ratios.

Conclusion

The effect of discontinuity dip direction was simulated in square and rectangular hard rock pillars, and the following conclusions can be made:

- If discontinuity dip angles below 45° are encountered, the advance of the excavation can be adjusted in a way such that the discontinuity dip direction is 45° to the pillar face. This will result in improved pillar strength compared to having the discontinuity parallel to the pillar faces. Conversely, the study shows that for steeper dip angles, the pillar strength may be compromised when the pillar faces are aligned at 45° to the discontinuity dip direction.
- The discontinuity dip factor (DDF) determined by Esterhuizen (2006) is based on discontinuities with dip directions that are parallel to the pillar faces. The results of this study can be used to modify the DDF for a dip direction of 45° relative to the pillar faces.
- The stability of rectangular pillars in the presence of discontinuities can be improved by aligning the long axis of the pillars at 0 to 45° with the discontinuity dip direction.

Limitations and future work

The proposed work was based on single set of properties, which can be used as a reference to develop other numerical models with different sets of properties.

The proposed work on pillar stability does not consider the influence of roof and floor failure.

This work demonstrates that further research through numerical modeling and field verification is needed to better quantify the strength of the pillars in the presence of discontinuities with different dip directions. The studies should include an assessment of the difference in strength of the pillars with increasing frequency of the discontinuities.

Disclaimer

The findings and conclusions in this paper are those of the authors and do not represent the views of NIOSH. Mention of any company name, product, or software does not constitute endorsement by NIOSH.

References

Dolinar, D.R., and Esterhuizen, G.S., 2007, "Evaluation of the effects of length on strength of slender pillars in limestone mines using numerical modeling," Proceedings of the 26th International Conference on Ground Control in Mining, Morgantown, WV, West Virginia University, pp. 304-313.

Esterhuizen, G.S., 1998, "Effect of Structural Discontinuities on Coal Pillar Strength as a Basis for Improving safety in the Design of Coal Pillar Systems," Safety in Mines Research Advisory Committee, COL 005a, December, 1998, pp. 1-104.

Esterhuizen, G.S., 2006, "An evaluation of the strength of slender pillars," Transactions of Society for Mining, Metallurgy & Exploration, Vol. 320, Society for Mining, Metallurgy & Exploration, Englewood, CO, pp. 69-76.

Esterhuizen G.S., Dolinar D.R., and Ellenberger J.L., 2008, "Pillar strength and design methodology for stone mines," Proceedings of the 27th International Conference on Ground Control in Mining. Morgantown, WV, West Virginia University, pp. 241-253.

Galvin J.M., Hebblewhite B.K., and Salamon M.D.G., 1999, "University of New South Wales coal pillar strength determinations for Australian and South African mining conditions," Proceedings of the Second International Workshop on Coal Pillar Mechanics and Design, Pittsburgh, PA, U.S. Publication No. 99-114, IC 9448, pp. 63-71.

Itasca Consulting Group, 2016, "Fast Lagrangian Analysis of Continua in 3 Dimensions," Minneapolis, MN.

Iannacchione, A.T., 1999, "Analysis of pillar design practices and techniques for U.S. limestone mines," Transactions of the Institution of Mining and Metallurgy, Section A: Mining Industry, Vol. 108, pp. A152-A160.

Jaeger, J.C., and Cook, N.G.W., 1979, Fundamentals of Rock Mechanics, 3rd Ed., Chapman and Hall, New York.

Kaiser, P.K., Diederichs, M.S., Martin, D.C., and Steiner, W., 2000, "Underground works in hard rock tunneling and mining, Keynote lecture," Geoeng2000, Melbourne, Australia, Technomic Publishing Co., pp. 841-926.

Lunder, P.J., and Pakalnis, R., 1997, "Determining the strength of hard rock mine pillars," Bulletin of Canadian Institute of Mining and Metallurgy, Vol. 90, pp. 51-55.

Madden, B.J., Canbulat, I., Jack, B.W., and Prohaska, G.D., 1995, "A Reassessment of Coal Pillar Design Procedures. Safety in Mines Research Advisory Committee," COL 021, December 1995, pp. 1-148.

Mark, C., and Chase, F.E., 1997, "Analysis of Retreat Mining Pillar Stability (ARMPS)," Seminar on New Technology for Ground Control in Retreat Mining, Pittsburgh, PA, U.S. Bureau of Mines, pp. 17-34.

Wagner, H., 1992, "Pillar design in South African collieries," Workshop on Coal Pillar Mechanics and Design, U.S. Bureau of Mines, IC 9315, pp. 283-301.